Electronic Supplementary Material (ESI) for RSC Advances.

Supporting Information

Temperature tuned syntheses of two new d^{10}-based Cd(II) cluster metal organic frameworks: Luminescent sensing and photocatalytic properties

Caiping Li,[a] Lu Lu,[a]* Jun Wang,[a] Qianqian Yang[b*], Deyun Ma,[c] Abhinav Kumar,[d*] Mohd. Muddassir,*[e] Ahmad Alowais,[e] and Naaser A. Y. Abduh[e]

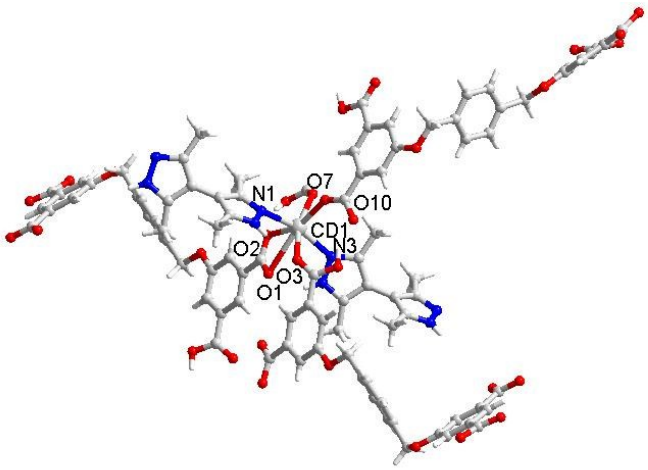

Fig. S1 view of the coordination environment of Cd(II) in **1**.

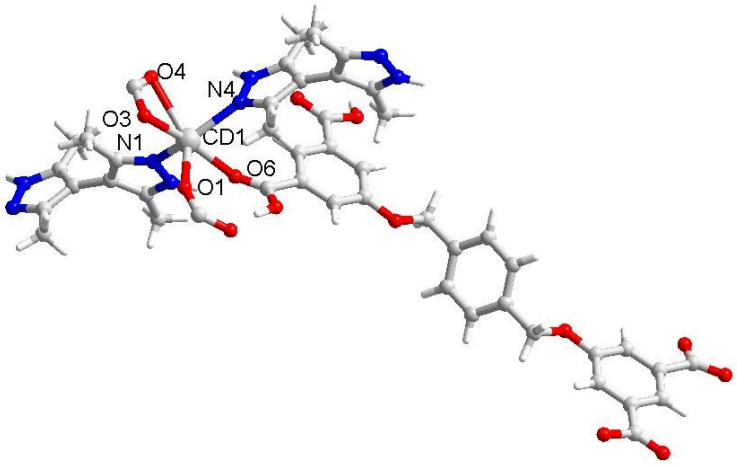

Fig. S2 view of the coordination environment of Cd(II) in **2**.

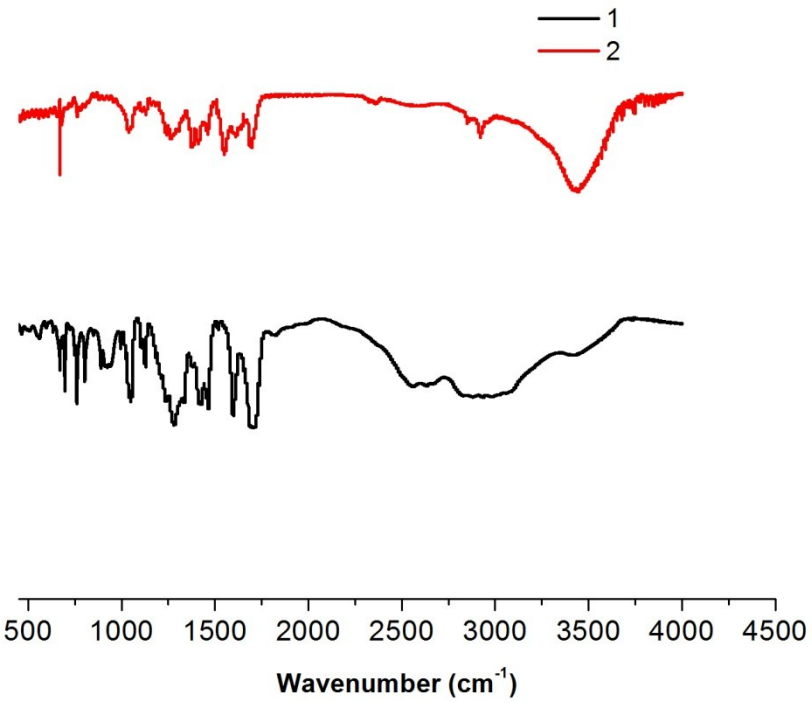

Fig. S3 FTIR spectra for MOFs **1** and **2**.

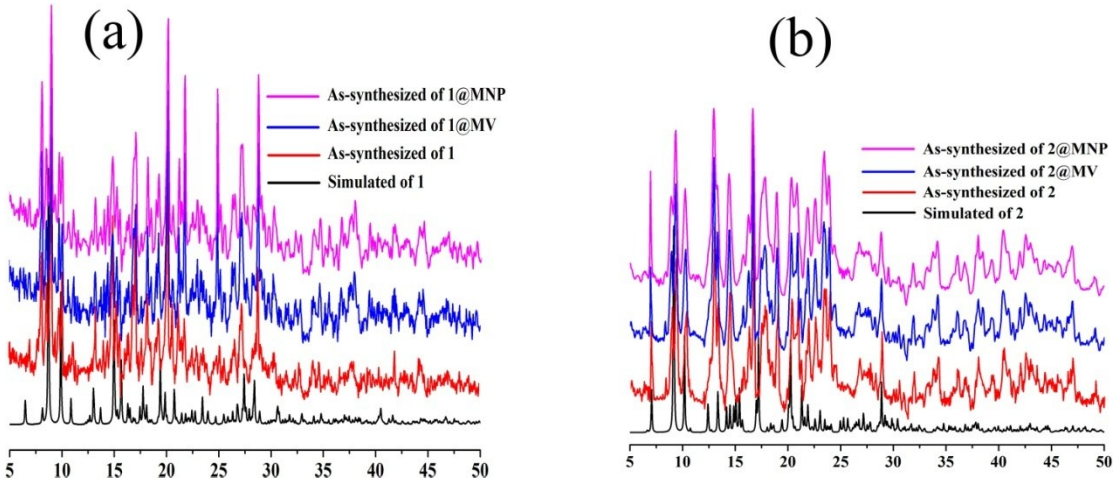

Fig. S4 Simulated PXRD patterns for **1** and **2** (black) obtained from single crystal data; PXRD patterns of as-synthesized compounds **1** and **2** (red); PXRD patterns of **1** and **2** isolated after photocatalysis of MV under UV light (blue) and PXRD patterns of **1** and **2** isolated after sensing of MNP (magenta).

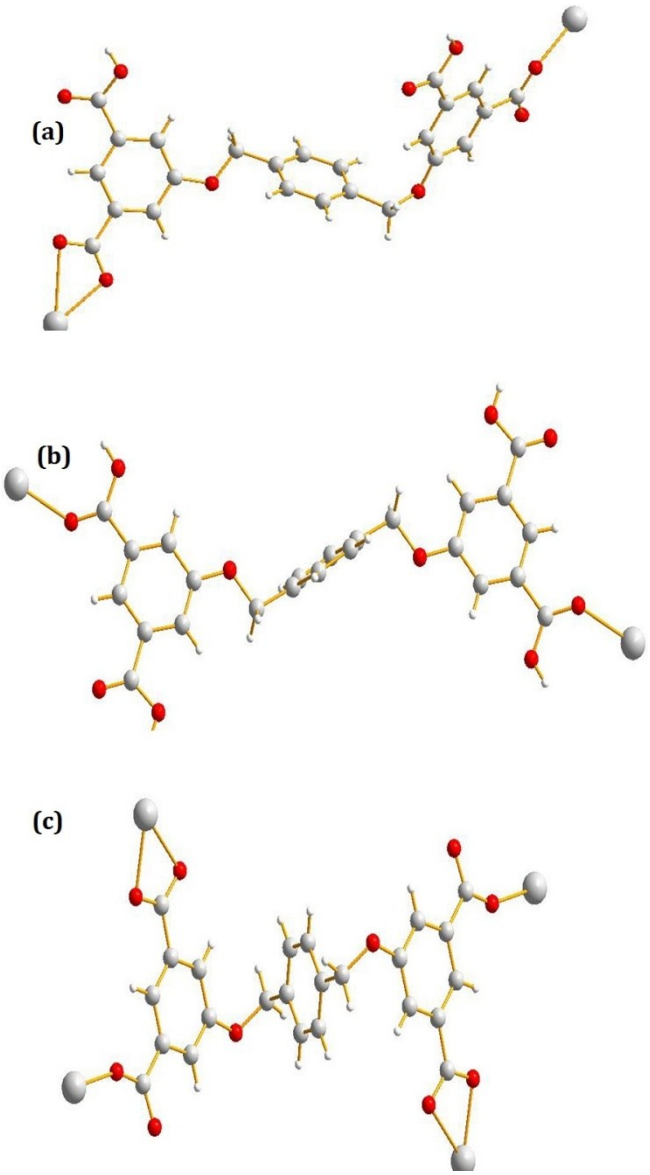

Scheme S1 view of the various coordination modes of H_4L in this work.

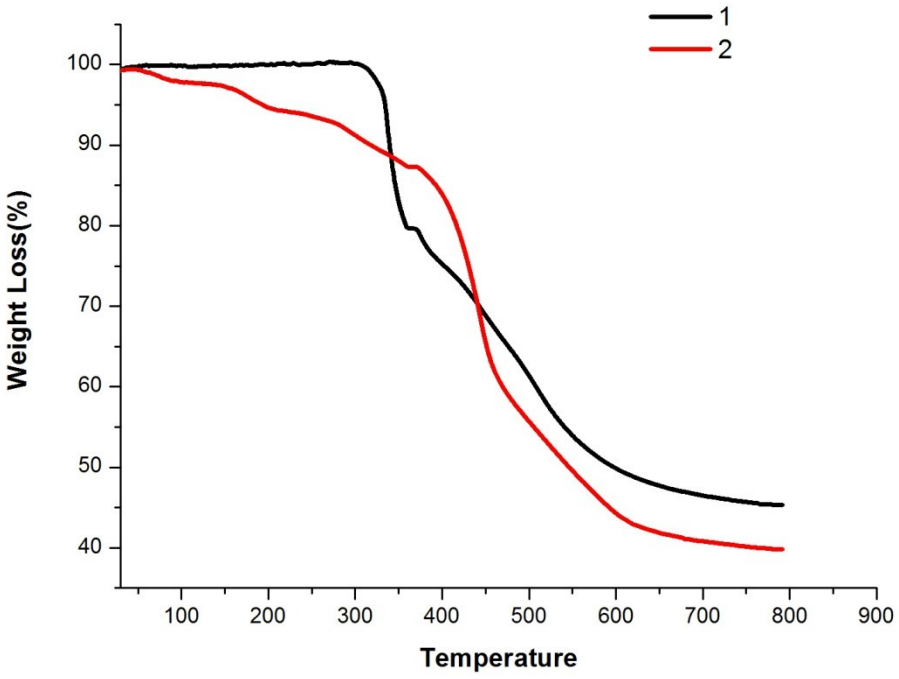

Fig. S5 TGA curves for MOFs **1** and **2**.

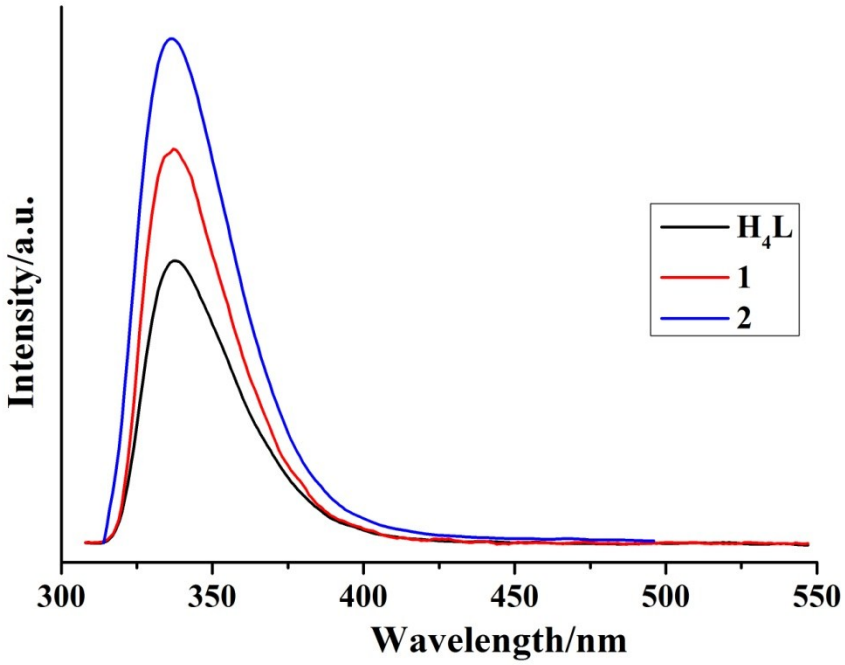

Fig. S6 PL intensities of H_4L ligand and title MOFs.

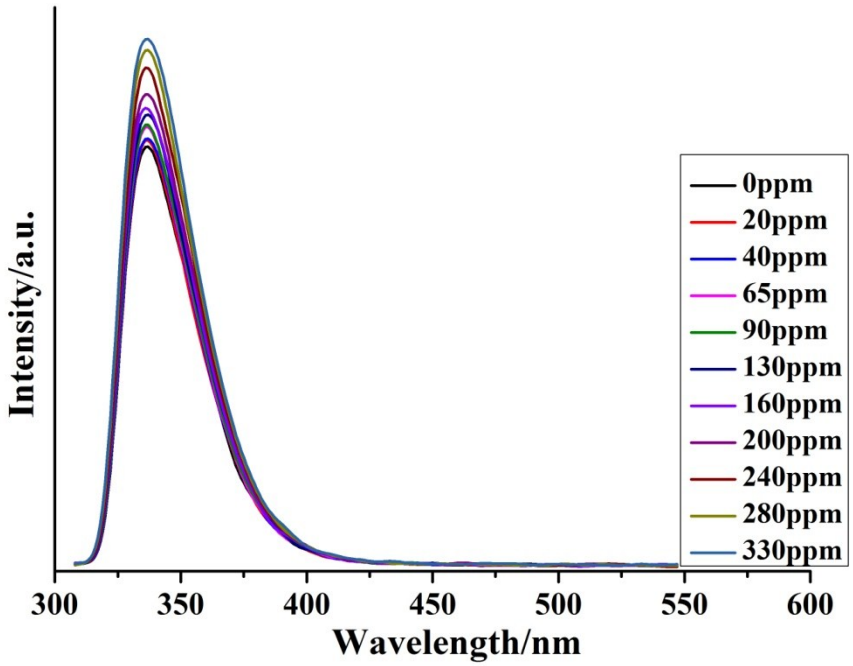

Fig. S7 Luminescent quenching of **1** dispersed in ethanol by the gradualaddition of 1 mM solution of 1,2,4-TMB.

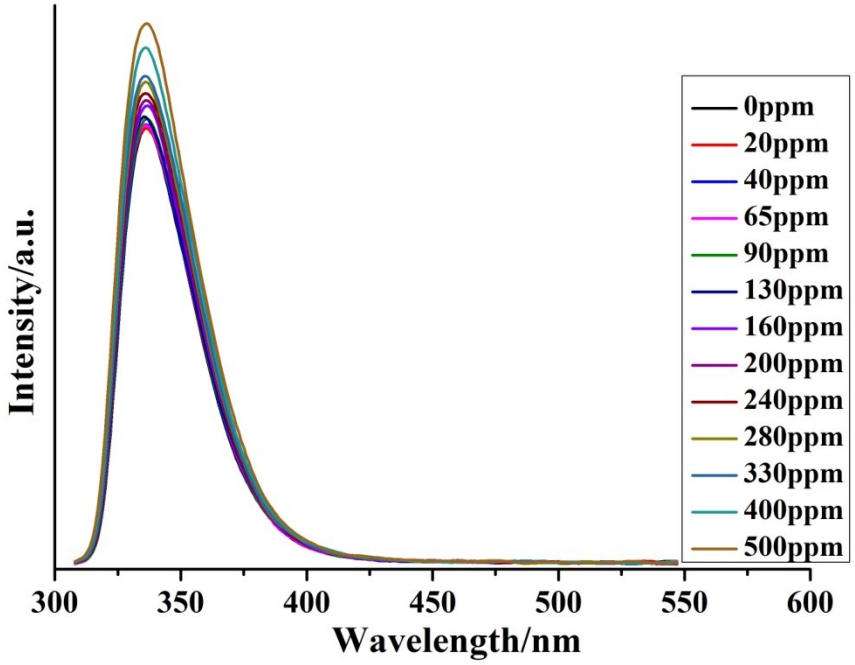

Fig. S8 Luminescent quenching of **1** dispersed in ethanol by the gradualaddition of 1 mM solution of 1,3,5-TMB.

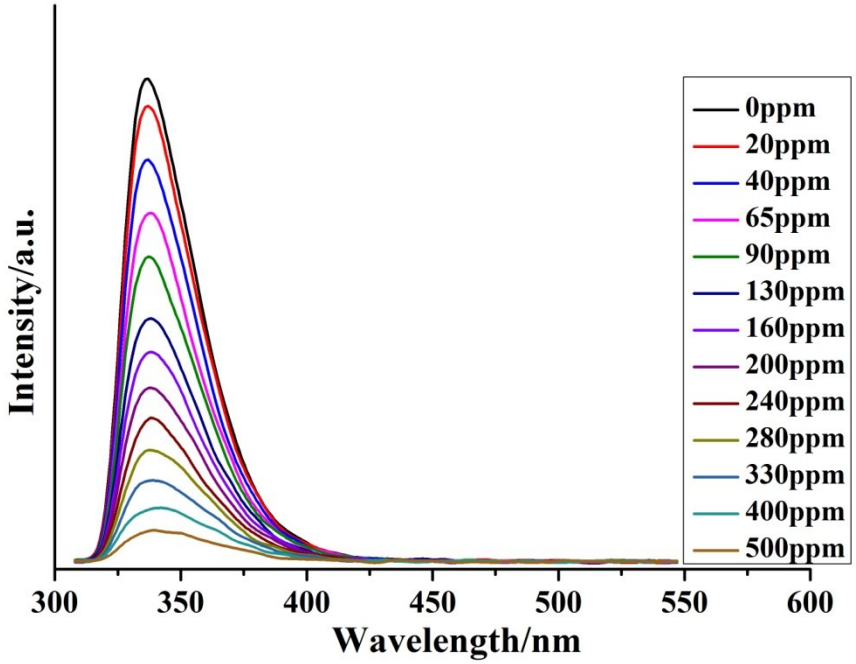

Fig. S9 Luminescent quenching of **1** dispersed in ethanol by the gradualaddition of 1 mM solution of 1,3-DNB.

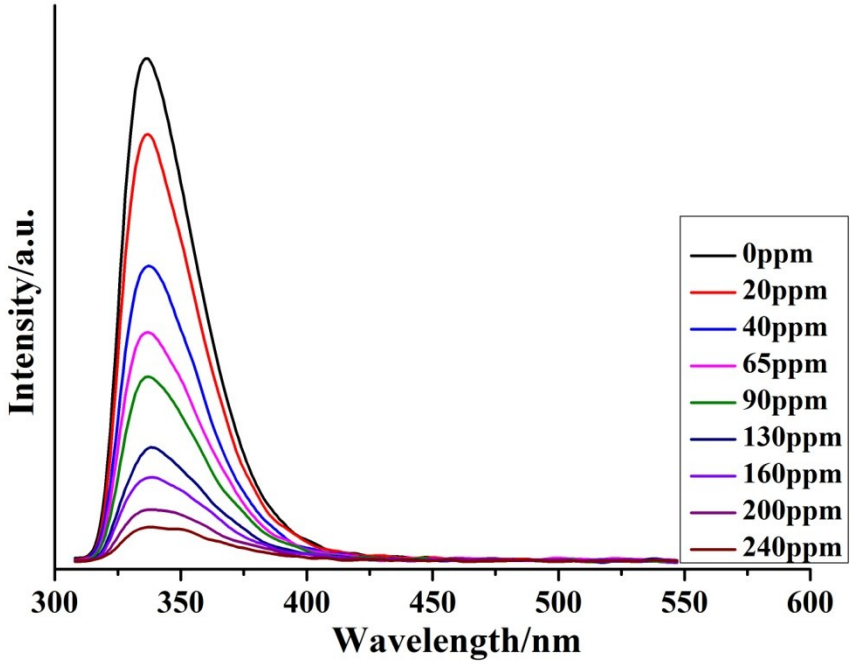

Fig. S10 Luminescent quenching of **1** dispersed in ethanol by the gradualaddition of 1 mM solution of 2,4-DNT.

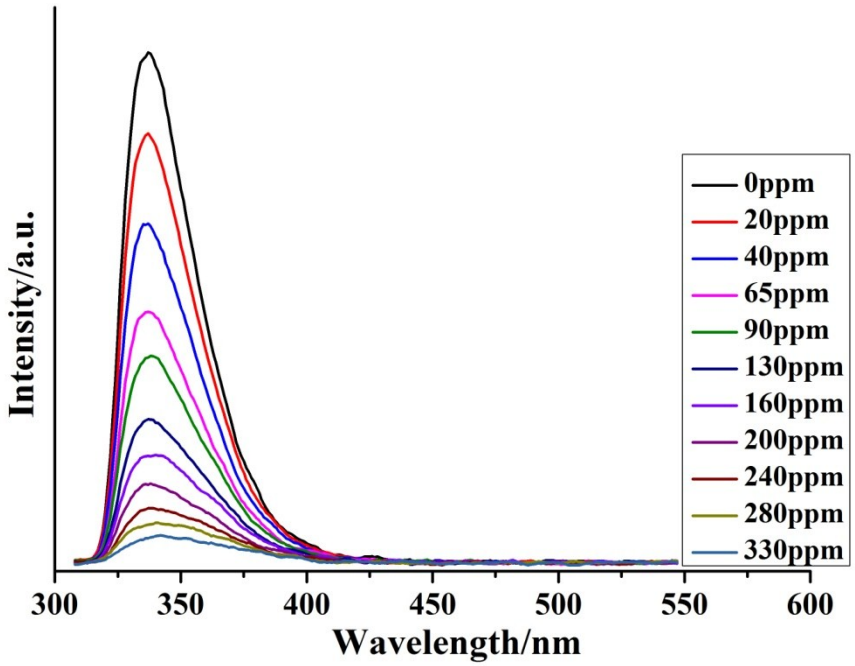

Fig. S11 Luminescent quenching of **1** dispersed in ethanol by the gradualaddition of 1 mM solution of 2,6-DNT.

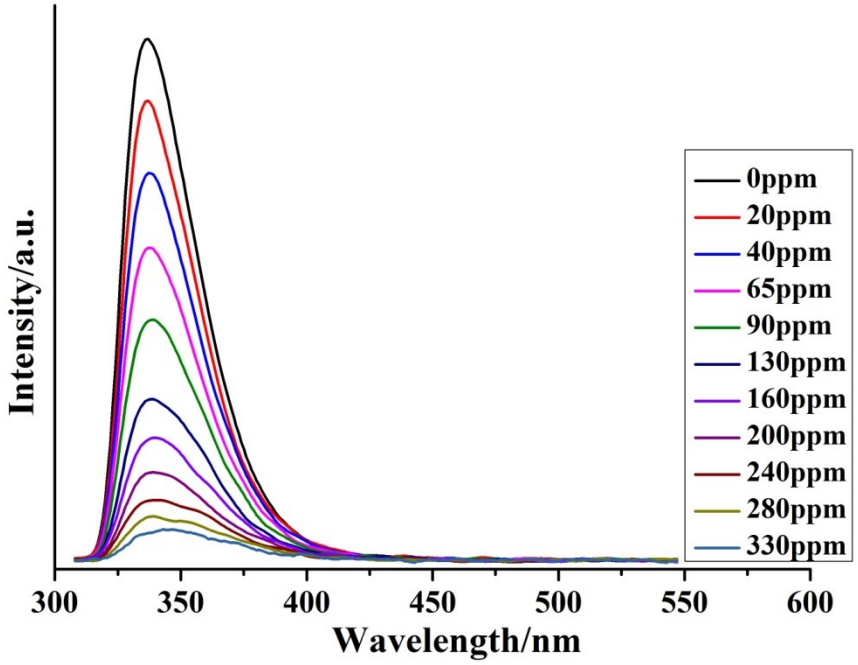

Fig. S12 Luminescent quenching of **1** dispersed in ethanol by the gradualaddition of 1 mM solution of 2-NT.

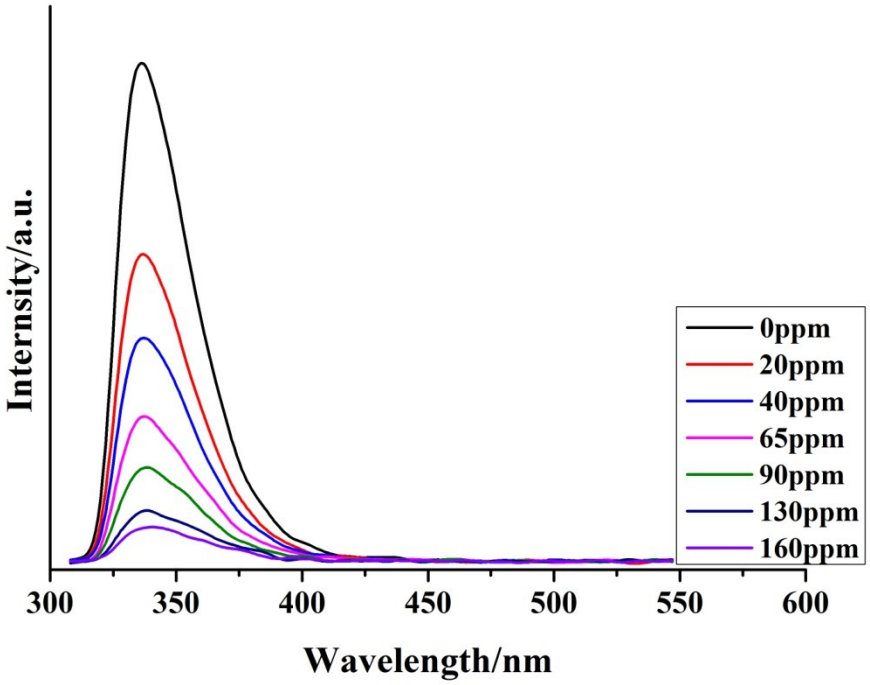

Fig. S13 Luminescent quenching of **1** dispersed in ethanol by the gradualaddition of 1 mM solution of 4-NT.

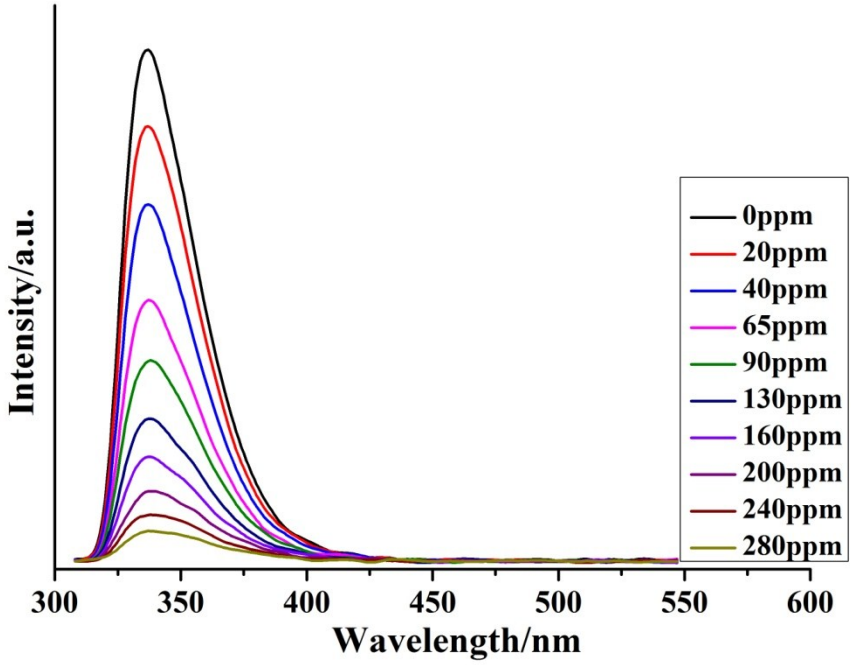

Fig. S14 Luminescent quenching of **1** dispersed in ethanol by the gradualaddition of 1 mM solution of NB.

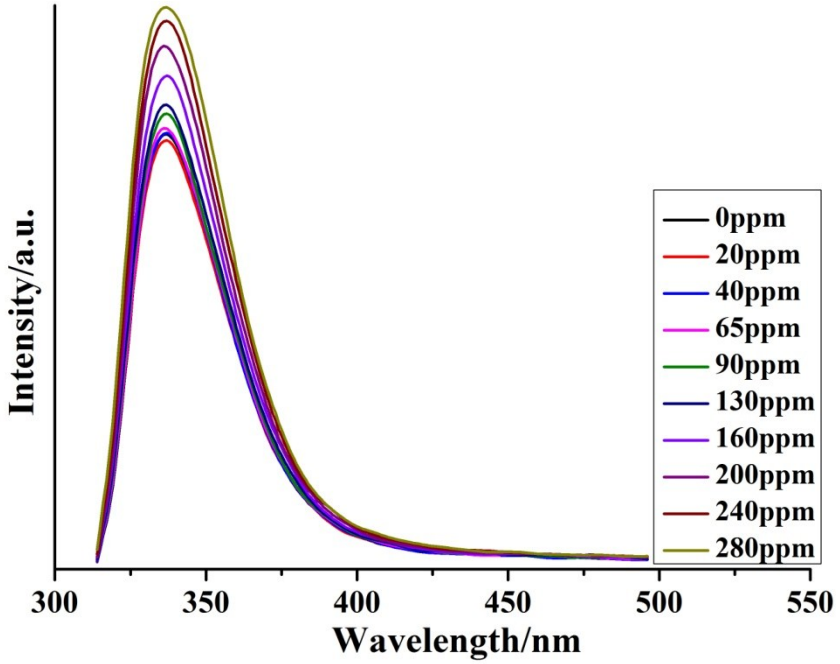

Fig. S15 Luminescent quenching of **2** dispersed in ethanol by the gradualaddition of 1 mM solution of 1,2,4-TMB.

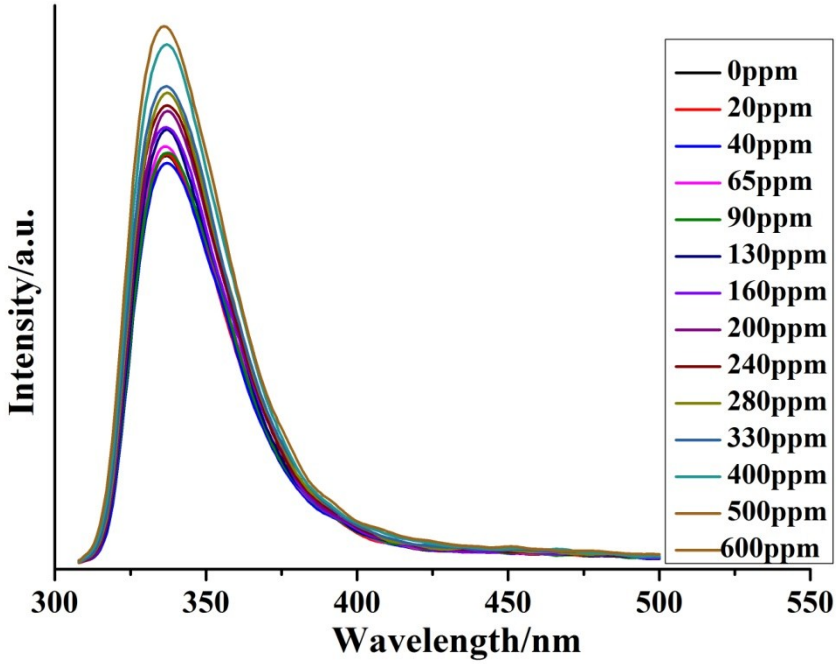

Fig. S16 Luminescent quenching of **2** dispersed in ethanol by the gradualaddition of 1 mM solution of 1,3,5-TMB.

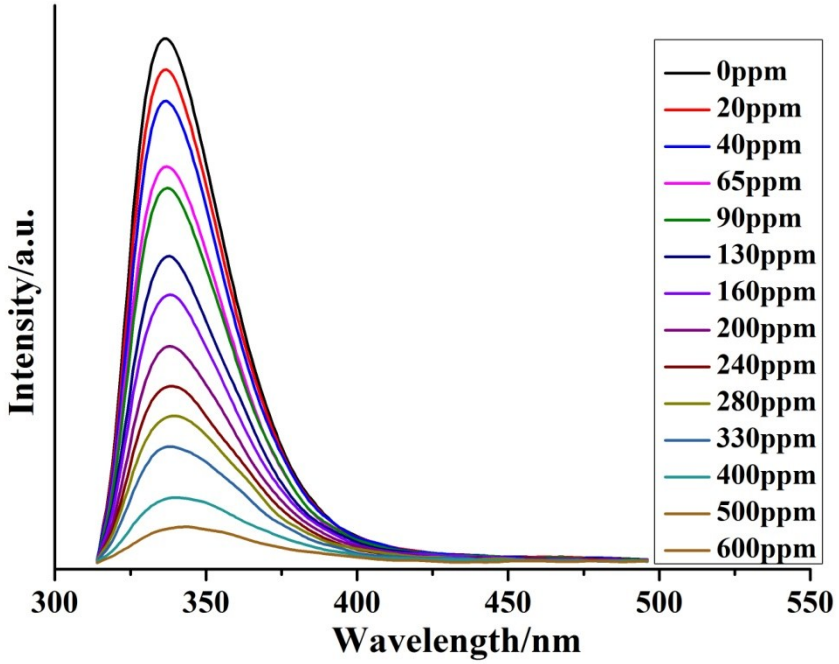

Fig. S17 Luminescent quenching of **2** dispersed in ethanol by the gradualaddition of 1 mM solution of 1,3-DNB.

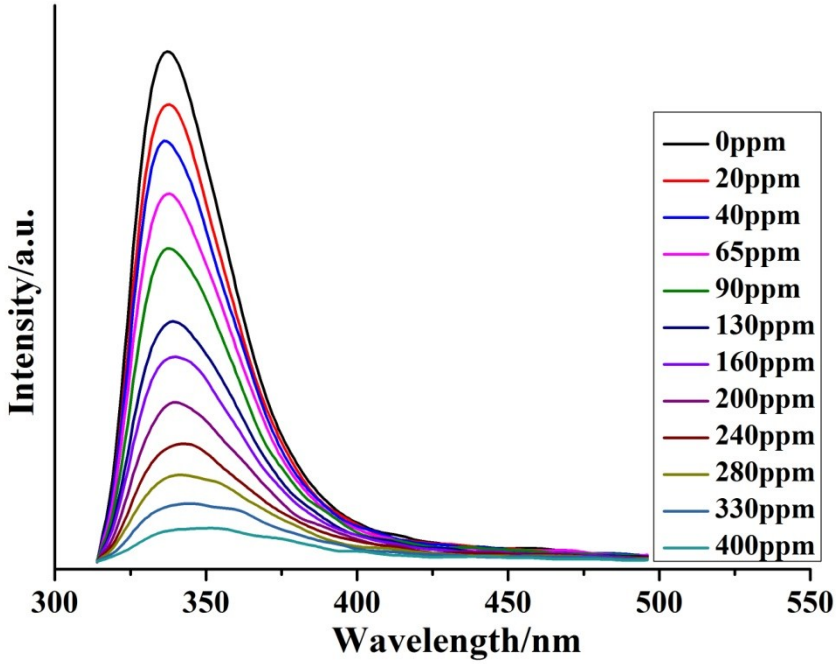

Fig. S18 Luminescent quenching of **2** dispersed in ethanol by the gradualaddition of 1 mM solution of 2,4-DNT

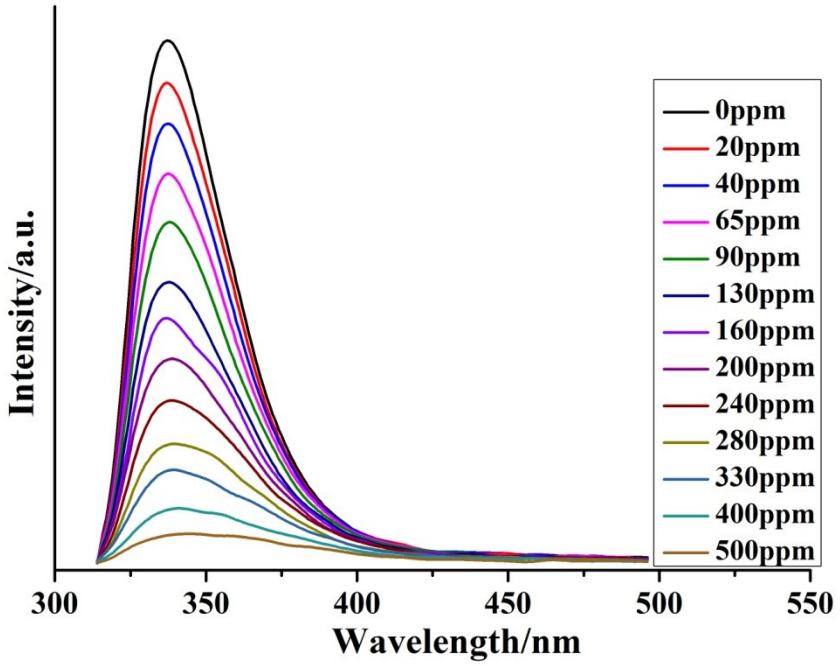

Fig. S19 Luminescent quenching of **2** dispersed in ethanol by the gradualaddition of 1 mM solution of 2,6-DNT.

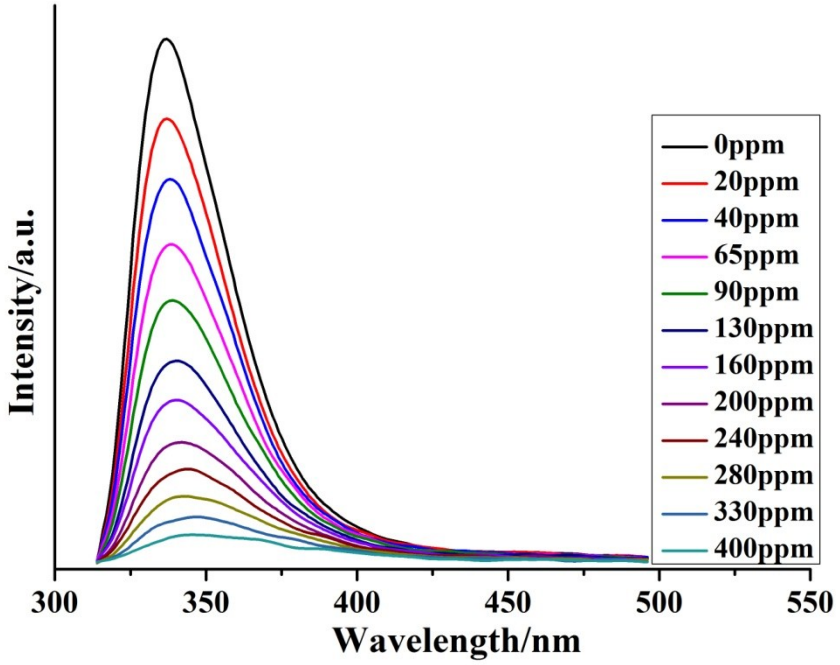

Fig. S20 Luminescent quenching of **2** dispersed in ethanol by the gradualaddition of 1 mM solution of 2-NT.

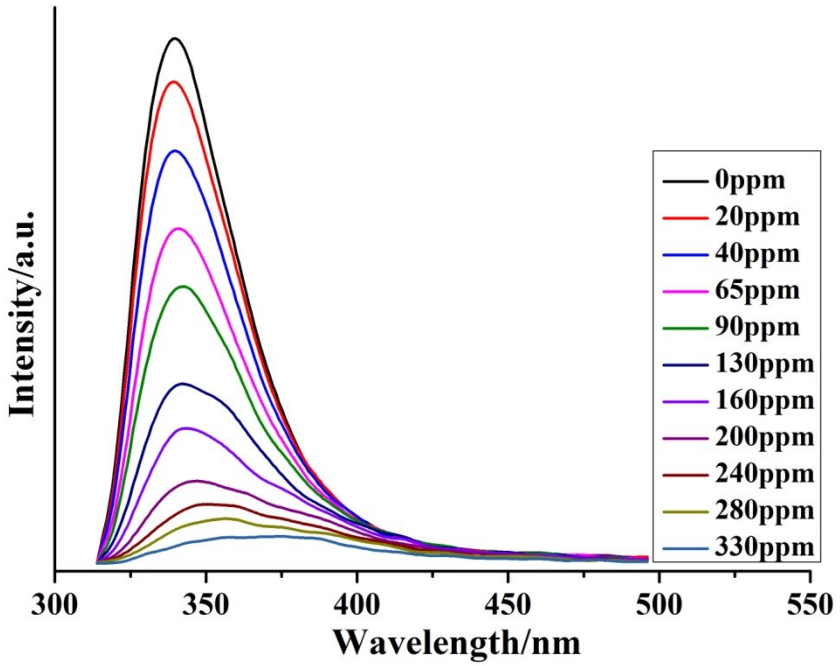

Fig. S21 Luminescent quenching of **2** dispersed in ethanol by the gradualaddition of 1 mM solution of 4-NT.

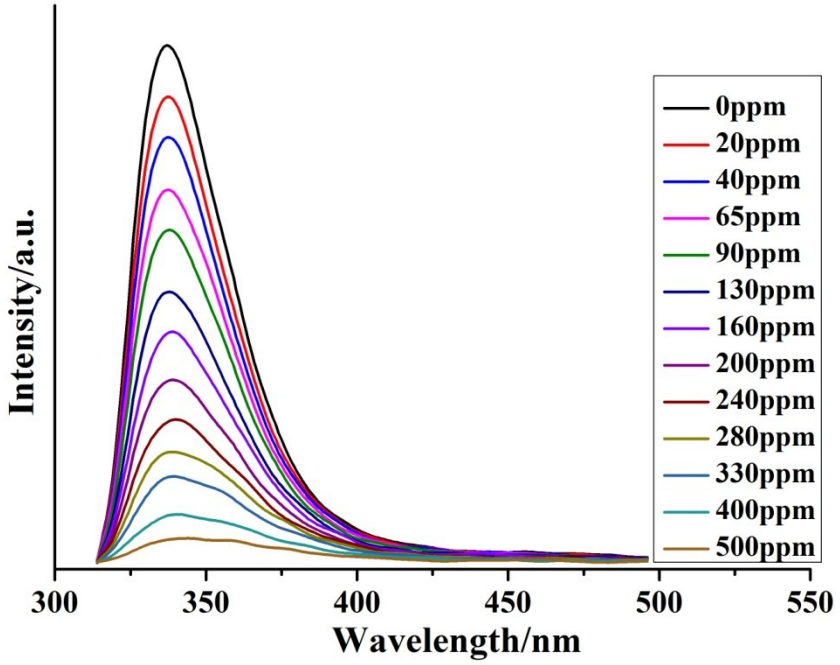

Fig. S22 Luminescent quenching of **2** dispersed in ethanol by the gradual addition of 1 mM solution of NB.

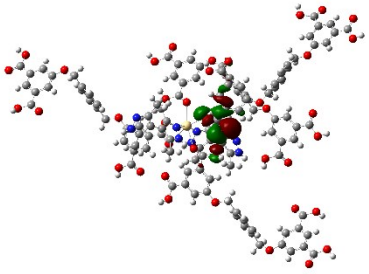

HOMO **1**

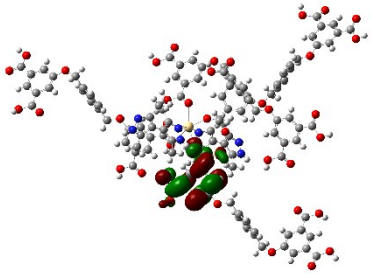

LUMO **1**

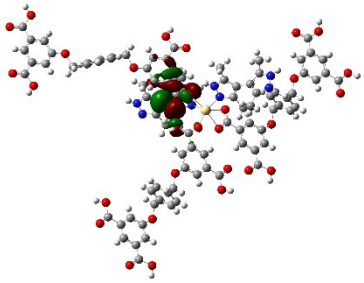

HOMO **2**

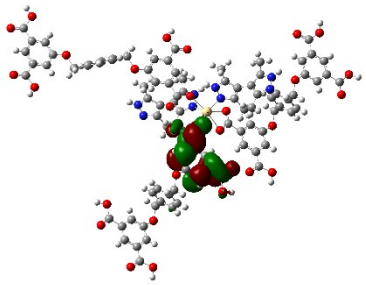

LUMO **2**

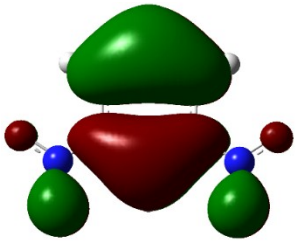

HOMO 1,3-DNB

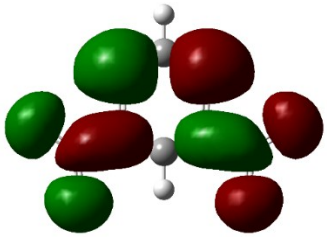

LUMO 1,3-DNB

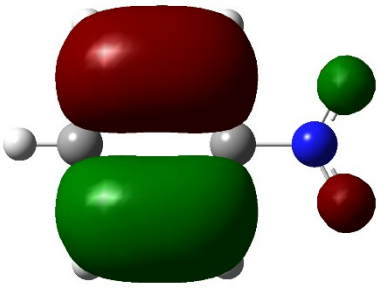

HOMO NB

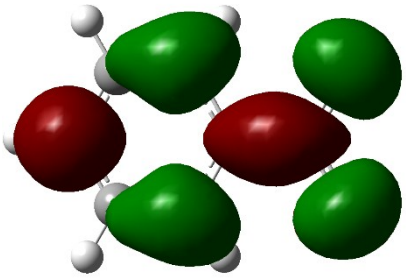

LUMO NB

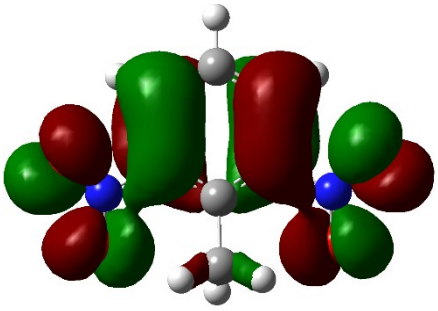

HOMO 2,6-DNT

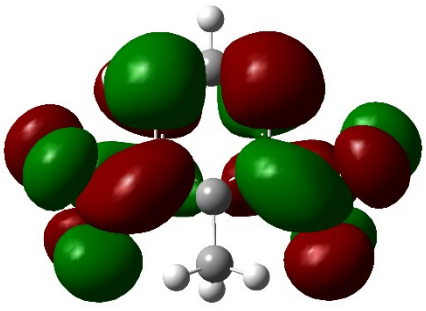

LUMO 2,6-DNT

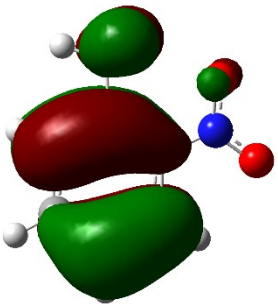

HOMO 2-NT

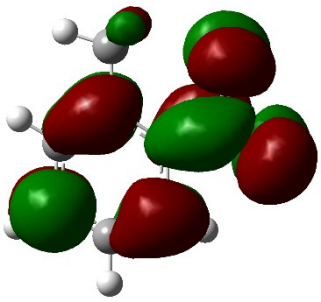

LUMO 2-NT

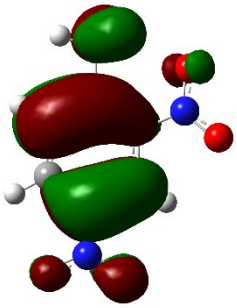

HOMO 2,4-DNT

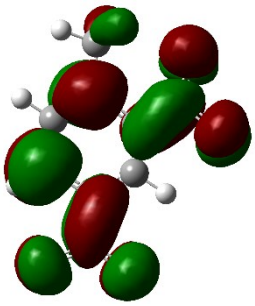

LUMO 2,4-DNT

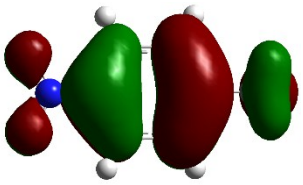

HOMO 4-NT

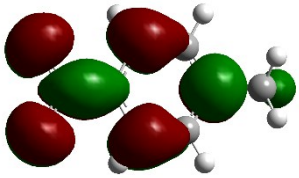

LUMO 4-NT

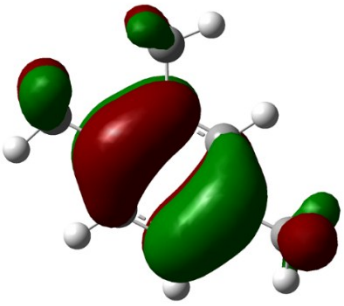

HOMO 1,2,4-TMB

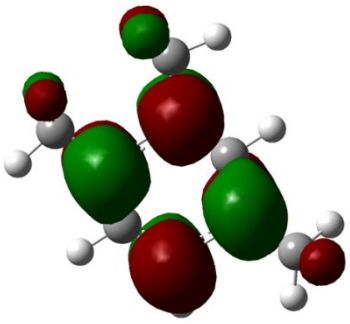

LUMO 1,2,4-TMB

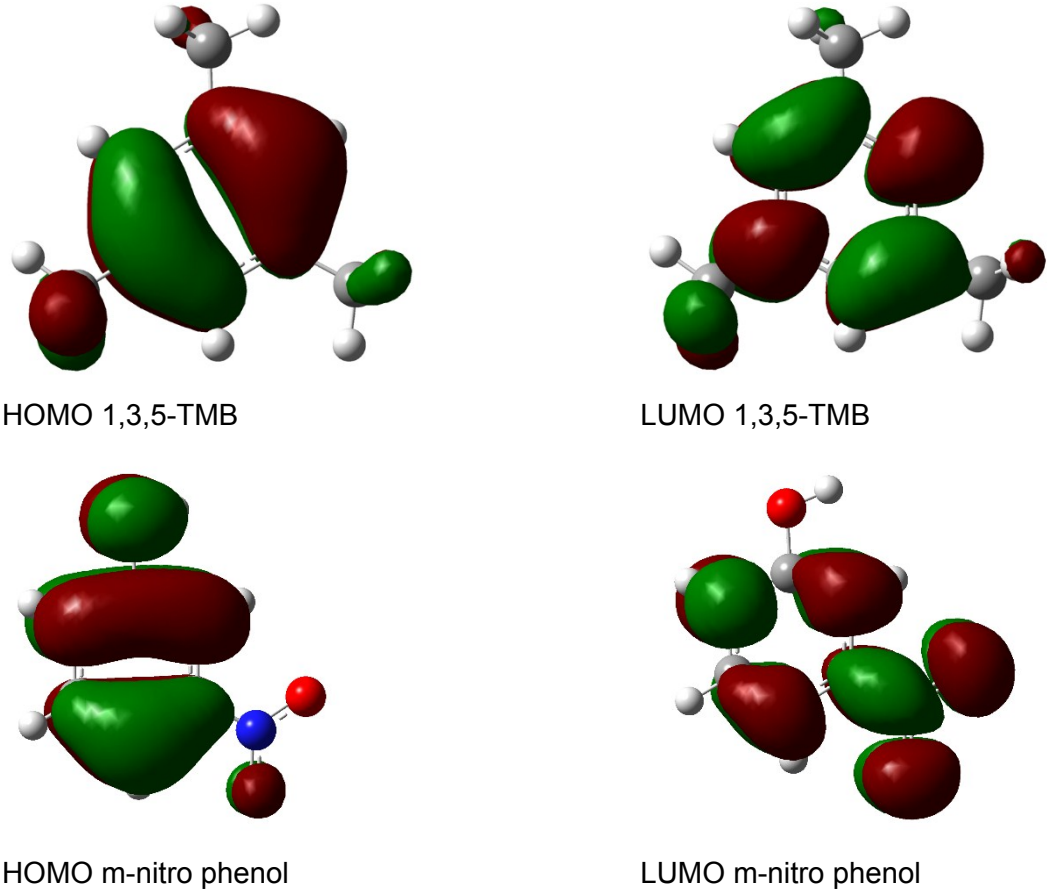

Fig. S23 HOMO-LUMO Plots for MOFs **1** and **2** as well as other analytes.

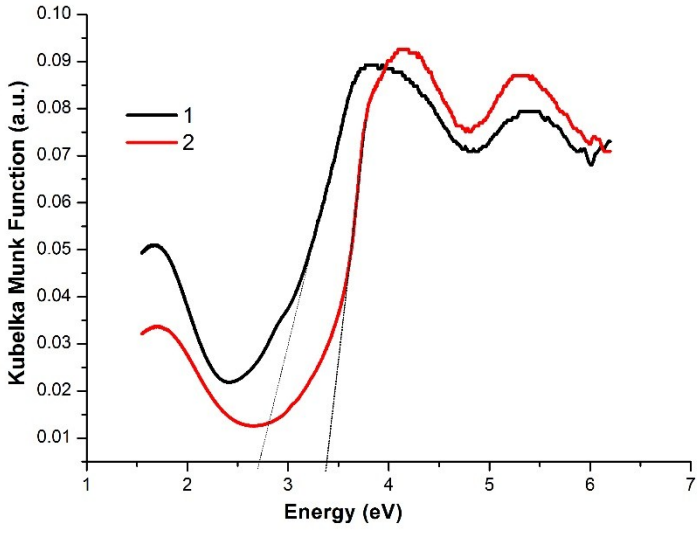

Fig. S24 The solid-state optical diffuse-reflection spectra for MOFs **1** and **2** derived from diffuse reflectance data at ambient temperature. The intercept of the extrapolated absorption edge on the energy scale (x axis) gives the band gap of the samples.

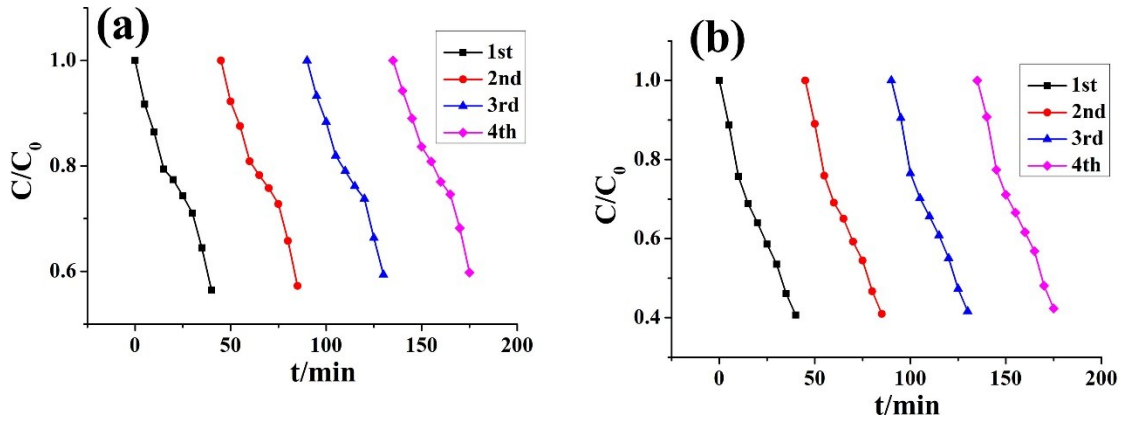

Fig. S25 Recycling tests of the photocatalytic degradation of MV by MOFs **1** (a) and **2** (b).

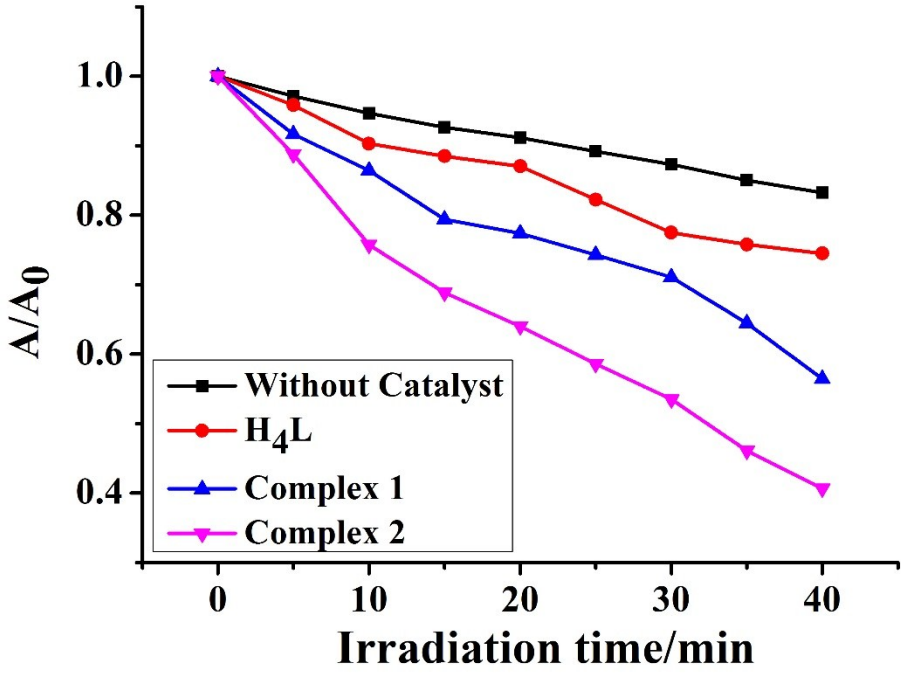

Fig. S26 Comparative photocatalytic efficiencies of MOFs, 1, 2, H_4L ligand for the photodegradation of MV under UV irradiation. Also, photodegradation of MV under control conditions without catalyst is presented.

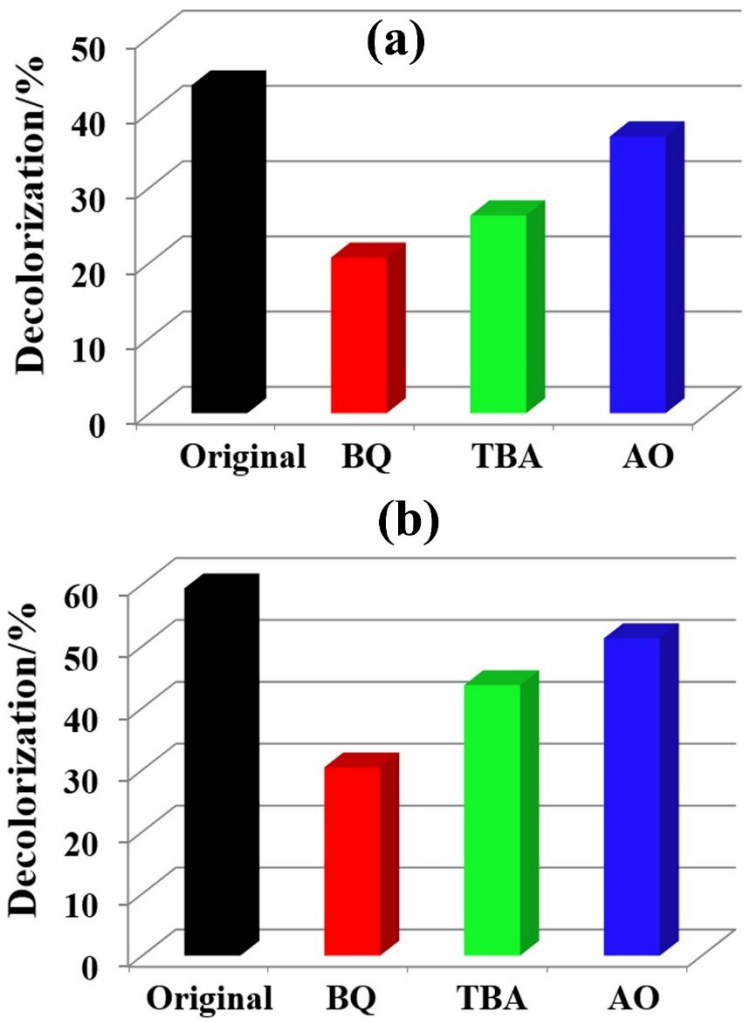

Fig. S27 The percentage degradation of MV under different conditions for **1** (a) and **2** (b).

Table S1. Crystallographic data and structure refinement details for MOFs 1-2

Parameter	**1**	**2**
Formula weight	767.02	767.02
Crystal system	Monoclinic	Triclinic
Space group	$P2_1/c$	*P-1*
Crystal Color	Yellow	Colorless
a, Å	10.205(3)	9.8116(9)
b, Å	27.207(7)	12.6840(12)
c, Å	11.915(3)	13.3634(13)
α, °	90	94.724(3)
β, °	95.979(4)	95.303(3)
γ, °	90	98.275(3)
V, Å ^{3}	3290.2(15)	1631.0(3)
Z	4	2
ρ_{calcd}, g/cm^3	1.548	1.562
μ, mm^{-1}	0.729	0.735
F(000)	1560	780
θ Range, deg	1.5-25.0	3.1-25.0
Reflection Collected	16248	29745
Independent reflections (R_{int})	0.060	0.110
Reflections with $I > 2\sigma(I)$	5791	5731
Number of parameters	446	450
R_1, wR_2 ($I > 2\sigma(I)$)*	0.0492, 0.1262	0.0487, 0.0715
R_1, wR_2 (all data)**	0.0718, 0.1507	0.0925, 0.0821

* $R = \sum(F_o - F_c)/\sum(F_o)$, ** $wR_2 = \{\sum[w(F_o^2 - F_c^2)^2]/\sum(F_o^2)^2\}^{1/2}$.

Table S2. Selected bond distances (Å) and angles (deg) for **1** and **2**

		1	
Cd(1)-O(2)	2.374(4)	Cd(1)-N(3)	2.280(4)
Cd(1)-N(1)$^{\#1}$	2.262(4)	Cd(1)-O(7)$^{\#2}$	2.475(4)
Cd(1)-O(3)$^{\#3}$	2.453(4)	Cd(1)-O(10)$^{\#4}$	2.249(4)
		2	
Cd(1)-O(1)	2.212(4)	Cd(1)-O(6)	2.390(3)
Cd(1)-N(4)	2.257(3)	Cd(1)-N(1)$^{\#1}$	2.268(3)
Cd(1)-O(3)$^{\#2}$	2.289(3)	Cd(1)-O(4)$^{\#2}$	2.552(3)
		1	
O(2)-Cd(1)-O(3)	96.36(15)	O(2)-Cd(1)-N(1)$^{\#1}$	86.32(16)
O(2)-Cd(1)-O(7)$^{\#2}$	86.32(16)	O(2)-Cd(1)-O(3)$^{\#3}$	118.14(12)
O(2)-Cd(1)-O(10)$^{\#4}$	150.80(14)	N(1)$^{\#1}$-Cd(1)-N(3)	160.89(17)
O(7)$^{\#2}$-Cd(1)-N(3)	89.48(14)	O(3)$^{\#3}$-Cd(1)-N(3)	80.70(13)
O(10)$^{\#4}$-Cd(1)-N(3)	96.92(16)	O(7)$^{\#2}$-Cd(1)-N(1)$^{\#1}$	109.48(16)
O(3)$^{\#3}$-Cd(1)-N(1)$^{\#1}$	81.37(15)	O(10)$^{\#4}$-Cd(1)-N(1)$^{\#1}$	89.51(16)
O(3)$^{\#3}$-Cd(1)-O(7)$^{\#2}$	163.52(12)	O(7)$^{\#2}$-Cd(1)-O(10)$^{\#4}$	78.35(13)
O(3)$^{\#3}$-Cd(1)-N(10)$^{\#4}$	89.66(13)		
		2	
O(1)-Cd(1)-O(6)	89.55(9)	O(1)-Cd(1)-N(4)	114.80(14)
O(1)-Cd(1)-N(1)$^{\#1}$	105.59(14)	O(1)-Cd(1)-O(3)$^{\#2}$	78.64(9)
O(1)-Cd(1)-O(4)$^{\#2}$	131.66(9)	O(1)-Cd(1)-O(8)$^{\#2}$	104.84(12)
O(6)-Cd(1)-N(4)	78.42(10)	O(2)-Cd(1)-N(1)$^{\#1}$	78.31(12)
O(3)$^{\#2}$-Cd(1)-O(6)	168.01(9)	O(4)$^{\#2}$-Cd(1)-O(6)	138.75(9)
O(6)-Cd(1)-C(8)$^{\#2}$	165.51(12)	N(1)$^{\#1}$-Cd(1)-N(4)	132.70(13)
O(3)$^{\#2}$-Cd(1)-N(4)	104.54(10)	O(4)$^{\#2}$-Cd(1)-N(4)	83.96(11)
N(4)-Cd(1)-C(8)$^{\#2}$	96.61(12)	O(3)$^{\#2}$-Cd(1)-N(1)$^{\#1}$	106.67(12)
O(4)$^{\#2}$-Cd(1)-N(1)$^{\#1}$	87.23(12))	O(3)$^{\#2}$-Cd(1)- O(4)$^{\#2}$	53.15(9)

Symmetry Codes: **For 1**: #1= -1+x, y, z; #2= 1+x, y, 1+z; #3= -1-x, -y, -z; #4= 1+x, 1/2-y, 3/2+z; **For 2**: #1 = 1+x, y, z; #2 = 2-x, 1-y, -z.

Table S3 LOD values for previously reported materials and MOFs 1 and 2 against MPN

Material	LOD	Ref
UiO-66-NH2	0.77	1
graphite	1049.643	2
montmorillonite	0.756	3
C/N-Au	0.74	4
calix[4]arene-bonded silica gels	2.8	5
NH_2-MCM-48	102.04	6
flay ash	8.06	7
organically modified diatomaceous earth	8.139	8
clinoptilolite	60	9
1	1.09	This work
2	0.81	This work

References:

1 Y. Dou, L. Guo, G. L. Li, X. X. Lv, L. Xia and J. You, Microchem. J. 2019, 146, 366–373

2 L. Y. Yu, X. W. Wu, Q. Liu, L. L. Liu, X. Y. Jiang, J. G. Yu, Chen, Feng, M. Zhong, J. Nanosci. Naonotech., 2016, 16, 12426-12432.

3. R. S. Juang, S. H. Lin and K. H. Tsao, J. Coll. Inter. Sci., 2004, 269, 46-52.

4. H. F. Zhou, S. X. Li, Y. J. Wu, D. J. Chen, Y. H. Li, F Y. Zheng and H. W. Yu, Sensors Actuators B, 2016, 237, 487–494

5 Y. E. Dolaksiz, F. Temel and M. Tabakci, React. Funct. Polymer, 2018, 126, 27–35

6 X.X. Gu, H. Kang, H. Li, X. C. Liu, F. Dong, M. Fu and J. R. Chen, *J. Chem. Eng. Data*20186393606-3614.

7 Singh, B. K.; Nayak, P. S. S, Sci. Technol. 2004, 22, 295−309.

8 Al Bakain, R. Z.; Abu-Zurayk, R. A.; Hamadneh, I.; Khalili, F. I.; Al-Dujaili, A. H. Water Treat. 2015, 56, 826−838.

9 Sismanoglu, T.; Pura, S. Colloids Surf. A 2001, 180,1−6.

Table S4 Performances of some MOFs used as photocatalysts for the degradation of MV under UV irradiation.

MOF	Irradiation	Degradation Efficiency (%)	ref
[Cd(4,4'-bpy)(H2O)2($S2O_3$)]	UV	99	1
[Cd_2(4,4'-bpy)$_{2.5}$(S_2O_3)$_2$]	UV	95	1
[Co_2(1,4-bdc)(ncp)$_2$]	Vis	33	2
[Cd(bidpe)(hmpa)]	UV	93	3
[Zn_2(L)(DMF)$_3$]	UV	72	4
1	UV	82	This work
2	UV	46	This work

References:

1 A. K. Paul, G. Madras and S. Natarajan, *Phys. Chem. Chem. Phys*., 2009, **11**, 11285–11296.

2 H.-Y. Sun, C.-B. Liu, Y. Cong, M.-H. Yu, H.-Y. Bai and G.-B. Che, *Inorg. Chem. Commun*., 2013, **35**, 130–134.

3 Z. A. Zong, C. B. Fan, C. F. Bi, X. Zhang, R. Luo, X. M. Meng, F. Jin and Y. H. Fan, *J. Solid, State. Chem*., 2019, **270**, 651-665.

4. J. C. Jin, J. Wu, Y. X. He, B. H. Li, J. Q. Liu, R. Prasad, A. Kumar and S. R. Battem, *CyrstEngComm*., 2017,**19**, 6464-6472